Three-level mixing and dark states in transport through quantum dots

Clive Emary, Christina Pöltl, and Tobias Brandes
Institut für Theoretische Physik, TU Berlin, Hardenbergstr. 36, D-10623 Berlin, Germany
(Received 27 August 2009; revised manuscript received 26 October 2009; published 16 December 2009)

We consider theoretically the transport through the double quantum dot structure of the recent experiment of Payette *et al.* [Phys. Rev. Lett. **102**, 026808 (2009)] and calculate stationary current and shot noise. Three-level mixing gives rise to a pronounced current-suppression effect, the character of which changes markedly with bias direction. We discuss these results in connection with the dark states of coherent population trapping in quantum dots.

DOI: 10.1103/PhysRevB.80.235321 PACS number(s): 73.63.Kv, 73.50.Td, 73.23.Hk

I. INTRODUCTION

In a recent experiment,[1] Payette *et al.* studied the transport through a double quantum dot (DQD) in which the source-side QD (QD1) had a single electronic level within the transport window, while the drain-side dot (QD2) possessed three (see Fig. 1). Gate voltages enabled the position of the former "*s* level" to be adjusted and thus used as a probe of the second QD. Due to nonellipticity, the levels of QD2 were found not to be the familiar Fock-Darwin (FD) levels,[2] but rather mixtures of them. This gave rise to a distinctive feature in the tunneling magnetospectrum consisting of an avoided crossing with a central line running through it. Strikingly, this central current line was not continuous as a function of magnetic field, as one might expect, but rather showed a strong suppression near the center of the avoided crossing. The authors of Ref. 1 suggested a connection between this phenomenon and that of the all-electronic coherent population trapping (CPT) of Refs. 3–6. It is the aim of this paper to explore this connection further.

We use a master equation treatment and calculate stationary current and shot noise. We consider a source-drain bias direction both as in Ref. 1 (forward bias), as well in the opposite direction (reverse bias). Both bias directions yield a current suppression, but as our calculations here reveal, the character is rather different in each case. In forward bias, the current-suppression valley is wide (proportional to the mixing energy between the levels) as observed in the experiment of Ref. 1 and the shot noise is sub-Poissonian. In the reverse-bias configuration, the current-suppression valley is narrow (proportional to the coupling rate with the leads) and the current statistics are strongly super-Poissonian. We argue that only in the latter case does the current blocking mechanism bear strong resemblance to coherent population trapping.

II. MODEL

We assume strong Coulomb blockade such that at most one excess electron can occupy the DQD at any one time and write the Hamiltonian of the complete system as

$$H = H_1 + H_2 + H_{12} + H_{\text{leads}} + V. \tag{1}$$

The Hamiltonian of the first dot reads $H_1=\varepsilon_s|s\rangle\langle s|$ with $|s\rangle$ denoting the single QD1 *s*-type orbital. Denoting the bare FD levels in the second dot as $|i\rangle$; $i=1,2,3$, we take the Hamiltonian of the second dot to be of the form

$$H_2 = E_B(|1\rangle\langle 1| - |3\rangle\langle 3|) + T(|1\rangle\langle 2| + |2\rangle\langle 1| + |2\rangle\langle 3| + |3\rangle\langle 2|), \tag{2}$$

where energy $E_B=c_B(B-B_0)$, with c_B a constant, describes the magnetic field dependence of the FD levels (here assumed linear for levels 1 and 3 and constant for level 2), and T is the coupling strength between the levels. We assume that the coupling between the two dots can be described by

$$H_{12} = \Omega\sum_{i=1}^{3}(|s\rangle\langle i| + |i\rangle\langle s|), \tag{3}$$

with common coupling parameter Ω. Finally, Hamiltonian $H_{\text{leads}}=\Sigma_{k,X}\varepsilon_{kX}c_{kX}^{\dagger}c_{kX}$ describes two standard fermionic reservoirs ($X=L,R$: left, right), and

$$V = \sum_k \left(V_{kL}c_{kL}^{\dagger}|0\rangle\langle s| + \sum_{i=1}^{3} V_{kR}c_{kR}^{\dagger}|0\rangle\langle i| \right) + \text{h.c.}, \tag{4}$$

with $|0\rangle$ the empty DQD state, describes the coupling of the dots to the leads. Note that here we have chosen the simplest configuration of parameters—our aim is the qualitative understanding of such systems and not the quantitative reproduction of the results of Ref. 1.

The eigenstates of Eq. (2) play the determining role in the transport through the system; we shall denote them $|\Psi_0\rangle$ and $|\Psi_{\pm}\rangle$, corresponding to eigenenergies $\varepsilon_0=0$ and

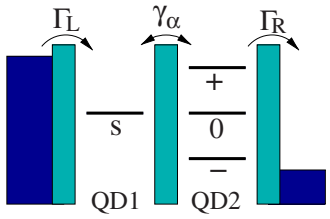

FIG. 1. (Color online) Double quantum dot with a bias window that includes the single probe *s* level in QD1 and three levels of QD2. The depicted bias configuration is as in Ref. 1, which we describe here as forward bias. In the sequential tunneling regime, electron tunneling is described by the rates Γ_L from left lead to QD1, Γ_R from QD2 to the right lead, and by γ_α; $\alpha=0,\pm$ between the dots.

$\varepsilon_\pm = \pm\sqrt{E_B^2+2T^2}$, such that $H_2|\Psi_\alpha\rangle = \varepsilon_\alpha|\Psi_\alpha\rangle$; $\alpha = 0, \pm$. The most important of these three states is that belonging to eigenvalue zero

$$|\Psi_0\rangle = |\Psi_0(E_B)\rangle = \frac{(-T|1\rangle + E_B|2\rangle + T|3\rangle)}{\sqrt{E_B^2+2T^2}}. \tag{5}$$

III. MASTER EQUATION

All three barriers of the double quantum dot are high, and thus a treatment in terms of Fermi's golden rule is appropriate for all tunneling in the system. Furthermore, we assume large bias such that, for a given bias direction, tunneling to/from the leads is unidirectional, and all relevant Fermi functions are either zero or one. We describe tunneling to/from left and right leads with the rates Γ_L and Γ_R, respectively. From the form of Eq. (4), the right-lead rates are the same for all three FD orbitals, and thus also for all three eigenstates $|\Psi_\alpha\rangle$.

Tunneling between the dots is governed by the matrix elements of H_{12} and, therefore, by the overlaps between the states in the two dots. Denoting the overlaps of the s level with the QD2 FD states as $\langle s|i\rangle = s_i$; $i=1,2,3$, we have, for example,

$$\langle s|\Psi_0\rangle = \frac{1}{\sqrt{E_B^2+2T^2}}[T(s_3-s_1)+E_B s_2]. \tag{6}$$

This eigenstate-overlap clearly vanishes for $E_B = T(s_1-s_3)/s_2$. In principle, overlaps s_i must be determined from calculation with orbital wave functions. However, here, we make the simple assumption that all s_i are the same. This is justified because the essential feature that $\langle s|\Psi_0\rangle$ vanishes remains regardless of the particular values of s_i. We then set these overlaps to unity, since they can be subsumed into the rate γ, to be defined below. The squares of the relevant matrix elements are then

$$|\langle s|\Psi_0\rangle|^2 = \frac{E_B^2}{E_B^2+2T^2} \tag{7}$$

$$|\langle s|\Psi_\pm\rangle|^2 = 1 + \frac{T^2}{E_B^2+2T^2} \pm \frac{2T}{\sqrt{E_B^2+2T^2}}. \tag{8}$$

Following Ref. 7, we then take the hopping rates between states s and α to be

$$\gamma_\alpha = \gamma|\langle s|\Psi_\alpha\rangle|^2 L(|\varepsilon_s - \varepsilon_\alpha|, \Gamma_L+\Gamma_R); \quad \alpha = 0, \pm, \tag{9}$$

where we have assumed a Lorentzian broadening of the levels, $L(x,w) = (1+(2x/w)^2)^{-1}$, and $\gamma = \gamma(\Omega)$ sets the overall scale for these rates.

With forward bias (as depicted in Fig. 1), the Liouvillian (rate matrix) of the system in a basis of populations of states ("empty," s, Ψ_0, Ψ_-, and Ψ_+) reads

$$\mathcal{L}_{\text{fwd}}(\chi) = \begin{pmatrix} -\Gamma_L & 0 & \Gamma_R & \Gamma_R & \Gamma_R \\ \Gamma_L e^{i\chi} & -\gamma_0-\gamma_--\gamma_+ & \gamma_0 & \gamma_- & \gamma_+ \\ 0 & \gamma_0 & -\gamma_0-\Gamma_R & 0 & 0 \\ 0 & \gamma_- & 0 & -\gamma_--\Gamma_R & 0 \\ 0 & \gamma_+ & 0 & 0 & -\gamma_+-\Gamma_R \end{pmatrix}. \tag{10}$$

In reverse bias, the right chemical potential lies above all three levels in QD2, with that on the left lying below the QD1 s level. The Liouvillian for this situation is

$$\mathcal{L}_{\text{rev}}(\chi) = \begin{pmatrix} -3\Gamma_R & \Gamma_L e^{i\chi} & 0 & 0 & 0 \\ 0 & -\Gamma_L-\gamma_0-\gamma_--\gamma_+ & \gamma_0 & \gamma_- & \gamma_+ \\ \Gamma_R & \gamma_0 & -\gamma_0 & 0 & 0 \\ \Gamma_R & \gamma_- & 0 & -\gamma_- & 0 \\ \Gamma_R & \gamma_+ & 0 & 0 & -\gamma_+ \end{pmatrix}. \tag{11}$$

Here, we have added counting field χ to facilitate the calculation of the current and shot noise.[9,10] The density matrix itself evolves under the action of the $\chi=0$ Liouvillian. For example, in the forward-bias case we have $\dot{\rho}(t) = \mathcal{L}_{\text{fwd}}(0)\rho(t)$. It should be noted that, although we have used the notation $\rho(t)$, only the diagonal elements of the system density matrix are actually included in this rate equation approach.[8]

Current statistics formalism

The current statistics of our model can straightforwardly be calculated using the jump-super-operator formalism of full counting statistics,[10–12] a brief review of which is given in the Appendix. In this notation, the stationary current and zero-frequency shot noise are given by

$$\langle I\rangle = \langle\langle \mathcal{J}\rangle\rangle \tag{12}$$

$$S = \langle\langle \mathcal{J}\rangle\rangle + 2\langle\langle \mathcal{J}\mathcal{R}(0)\mathcal{J}\rangle\rangle. \tag{13}$$

We further define the Fano factor as $F = S/\langle I\rangle$.

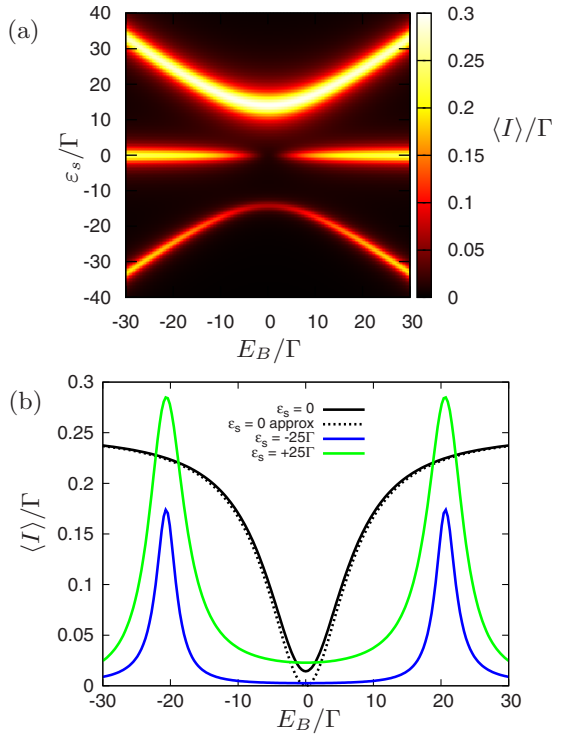

FIG. 2. (Color online) Current through the DQD in the forward-bias configuration: (a) density plot as a function of magnetic energy E_B and s-level position ε_s. (b) sections at $\varepsilon_s=0$, $\varepsilon_s=-25\Gamma$, and $\varepsilon_s=25\Gamma$. Also plotted (dashed) is the approximate current of Eq. (14) (for $\varepsilon_s=0$). A strong current suppression is observed around the point $\varepsilon_s=E_B=0$, but note that a small current does flow at this point, however. Here, we set $\Gamma_L=\Gamma_R=\Gamma$ as in the text, and also $\gamma=\Gamma$ and $T=10\Gamma$.

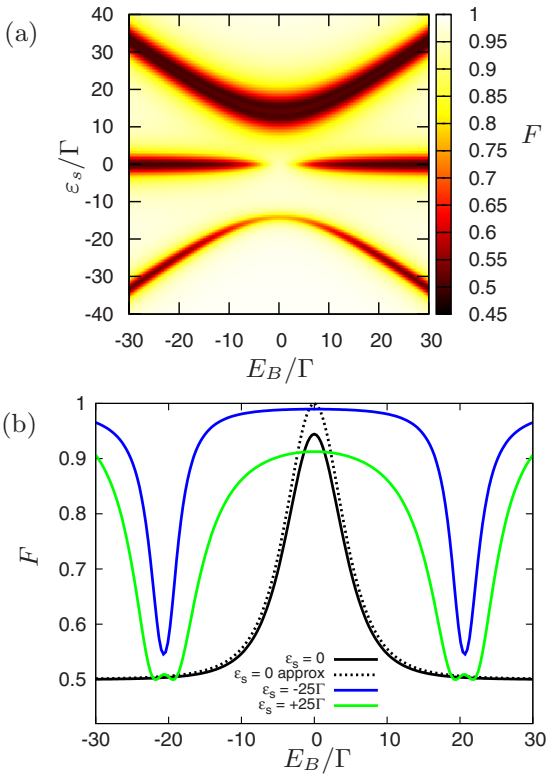

FIG. 3. (Color online) As Fig. 2, but here, the shot noise Fano factor is shown. Along the resonant lines of high current, the shot noise is sub-Poissonian with a Fano factor $F\approx 1/2$. Away from resonance, as well as around the central current-suppression region, the shot noise approaches the Poissonian value $F=1$ from below.

IV. RESULTS

In all the following, we set $\Gamma_L=\Gamma_R=\Gamma$ for ease of presentation. Furthermore, in the experiment all tunneling rates were much smaller that the level-mixing strength, $\gamma \ll T$, and we will use this fact in various approximate results.

A. Forward bias

Figure 2 shows the current through the system as a function of magnetic energy E_B and QD1 level position, ε_s. The general structure of the measurements of Ref. 1—an avoided crossing with a line through the middle—is reproduced, with current suppression near $\varepsilon_s=E_B=0$ clearly present. Near this point, the s level is close to resonance with the QD2 state $|\Psi_0\rangle$ and, if we ignore contributions from the other two levels, the current through the system may be approximated as that flowing through state $|\Psi_0\rangle$ alone

$$\langle I\rangle_{\rm fwd} \approx \frac{\gamma_0\Gamma}{\Gamma+3\gamma_0}. \tag{14}$$

The rate γ_0 is proportional to the matrix element $|\langle s|\Psi_0\rangle|^2$, which from Eq. (7) is seen to vanish at $E_B=0$. Within this approximation, the stationary state of the system at $\varepsilon_s=E_B=0$ is $\rho_{\rm stat}=|s\rangle\langle s|$, with an electron trapped in the s level due to the vanishing of the matrix element. In this approximation, the current at this point is zero. From Fig. 2(b), however, it is clear that the current is not completely suppressed at $\varepsilon_s=E_B=0$, but is finite due to the conduction through the other two states $|\Psi_\pm\rangle$. This residual current can be estimated as $I_{\rm fwd}\approx 3\gamma\Gamma^2/(2T^2)$, which need not be negligible.

The width of current-suppression feature at $\varepsilon_s=0$ can be approximated as follows. Close to $E_B=0$, γ_0 is small, and Eq. (14) can be further approximated as $I_{\rm fwd}\approx\gamma_0$. On the other hand, far from $E_B=0$, the current saturates to the constant value $I_{\rm fwd}\approx\Gamma\gamma/(3\gamma+\Gamma)$. The value of the magnetic field at the point where these two behaviors cross can be found by setting the two limiting values equal, and solving for E_B. Equating this value to half the width of the current-suppression valley, we find

$$w_{\rm fwd}=\sqrt{\frac{8\Gamma}{3\gamma}}T, \tag{15}$$

which shows the width of the current-suppression valley to be proportional to the level-mixing energy T.

The shot noise Fano factor for this bias direction is shown in Fig. 3. Especially evident is that, the Fano factor is everywhere less than (or equal to) unity, corresponding to the familiar sub-Poissonian statistics of antibunched electron transfer. Again assuming that only the central resonance determines the transport in the neighborhood of the current suppression, we can approximate

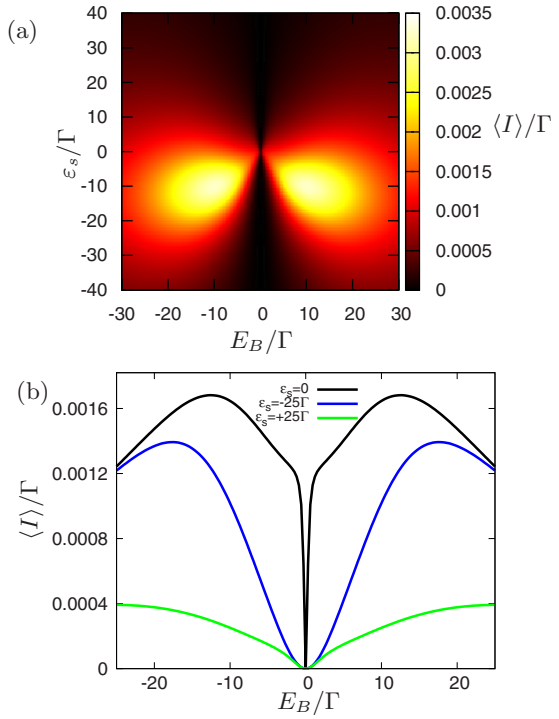

FIG. 4. (Color online) Current in the reverse bias, parameters as Fig. 2. Here, the level structure of the second dot is not resolved. Rather, two large current peaks are observed. Along the E_B=0 axis, the current is completely suppressed, irrespective of the s-level position. This is attributed to the formation of the CPT dark state of Eq. (17).

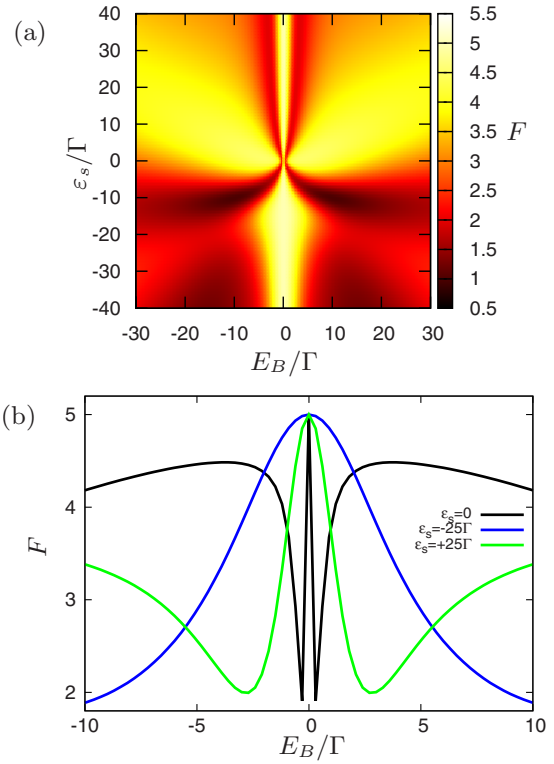

FIG. 5. (Color online) Shot noise Fano factor in the reverse bias, parameters as Fig. 3. In contrast to the forward-bias case, the shot noise is almost everywhere super-Poissonian. For E_B=0, the Fano factor is exactly 5.

$$F_{\mathrm{fwd}} \approx \frac{\Gamma^2 + 2\Gamma\gamma_0 + 5\gamma_0^2}{(\Gamma + 3\gamma_0)^2}, \tag{16}$$

which is clearly always less than or equal to unity. Along the central resonance (ε_s=0), the Fano factor reaches a maximum value $F \approx 1 - 6\gamma\Gamma/T^2$ at E_B=0 and a limiting value of $F \approx (5\gamma^2 + 2\gamma\Gamma + \Gamma^2)/(\Gamma + 3\gamma)^2$ for large E_B along the ε_s=0 line.

B. Reverse bias

Figure 4 shows the current with the source-drain bias in the opposite direction. Once again, the current shows suppression at E_B=0, but unlike the forward-bias case, this suppression extends for all positions of the s level. The second significant feature of this suppression is that, the current is *exactly* zero at E_B=0, even for T/γ finite. It is easily shown that for E_B=0, the stationary density matrix of the system is $\rho_{\mathrm{stat}} = |\Psi_0(0)\rangle\langle\Psi_0(0)|$, which clearly shows that in the long-time limit, an electron is trapped in the DQD in the pure state

$$|\Psi_0(0)\rangle = \frac{1}{\sqrt{2}}(|3\rangle - |1\rangle). \tag{17}$$

We can obtain an approximation to the exact expression for the current as follows. If Γ and γ are on the same order of magnitude, then, for any choice of ε_s, at least one of γ_α will be much smaller than Γ. We can then write the current as

$$I_{\mathrm{rev}} \approx \frac{3\gamma_0\gamma_+\gamma_-}{\gamma_0\gamma_+ + \gamma_0\gamma_- + \gamma_+\gamma_-}. \tag{18}$$

Concentrating about the point ε_s=0, we can say that near E_B=0 there is always a regime in which γ_0 is the smallest rate (matrix element disappears). In this case, the current becomes $I_{\mathrm{rev}} \approx 3\gamma_0$. This expression describes the form on the sharp dip in the current about E_B=0. Further away from E_B=0, γ_0 becomes the largest of the γ_i rates since its matrix element returns to a typical nonsuppressed value and the other two rates are off-resonant. In this case, the current becomes $I_{\mathrm{rev}} \approx 3\gamma_+\gamma_-/(\gamma_+ + \gamma_-)$. An estimate of the width of the current-suppression feature can then be obtained from the crossover between these two behaviors that occurs when $\gamma_0 = \gamma_+$ (N.B.: for ε_s=0, $\gamma_- < \gamma_+$). Solving for E_B, we find the width to be

$$w_{\mathrm{rev}} = \sqrt{6 + 4\sqrt{2}}\Gamma, \tag{19}$$

which is proportional to the broadening induced by the contacts.

The corresponding Fano factor is shown in Fig. 5. In strong contrast to the forward-bias case, the noise here is almost everywhere super-Poissonian, and in particular in the neighborhood of the current suppression. Under the same approximation that led to Eq. (18), the Fano factor is

$$F_{\mathrm{rev}} \approx \{5(\gamma_0^2\gamma_+^2 + \gamma_0^2\gamma_-^2 + \gamma_+^2\gamma_-^2) - 2\gamma_0\gamma_+\gamma_-(\gamma_0 + \gamma_+ + \gamma_-)\} \times \{\gamma_0\gamma_+ + \gamma_0\gamma_- + \gamma_+\gamma_-\}^{-2}. \quad (20)$$

From this form, it is clear that at $E_B=0$, $\gamma_0=0$, and the Fano factor is simply $F=5$, independent of all further parameters. This remains true of the full expression for F_{rev} (too unwieldy to show here), and for any choice of Γ_L, Γ_R, and γ, even if the interdot tunneling amplitudes are different. In this respect, the existence of this reverse-bias blocking mechanism, with the associated value of five for the Fano factor, is rather robust.

V. DISCUSSION

The foregoing results allow us to form a physical picture of the transport mechanisms at work in the current suppression here.

For forward bias, near the point $\varepsilon_S=E_B=0$, conduction comes through three channels that are weakly transmitting: two ($\pm$) on account of their distance in energy from resonance with the probe level at ε_s, and one (0) on account of the vanishing of the matrix element for hopping between the two dots. In this case, the steady state of the DQD is approximately that of an electron trapped in the QD1 probe-level $\rho_{\mathrm{stat}} \approx |s\rangle\langle s|$. This trapping is not exact, however, and a current still flows at $\varepsilon_S=E_B=0$ due to conduction through the off-resonant channels. As there is only a single path for the electrons to enter the DQD, there is no opportunity for any interaction-induced bunching of the electrons. The resulting statistics are, therefore, sub-Poissonian, as one would obtain from a noninteracting system.[13] This situation resembles somewhat the isospin blockade of Ref. 14.

In contrast, the current in the reverse direction for $E_B=0$ is exactly zero—not just for $\varepsilon_s=0$, but irrespective of probe-level position. In this case, the dot electron is trapped in the state: $2^{-1/2}(|3\rangle - |1\rangle)$. This is a pure superposition state and is directly analogous to the dark state of the triple quantum dot CPT.[3] As in the triple dot case, the corresponding current statistics are super-Poissonian. This may be understood in terms of the dynamical channel blockade,[15] since we have one weakly transmitting channel (that associated with the dark state), and two normally conducting ones.

A further distinguishing feature between these two blockade situations is that the width of the forward-bias suppression valley is proportional to the mixing amplitude T (the large energy scale in the model), whereas that in reverse bias is proportional to the lead-coupling rate Γ (the small energy scale). We also mention that the reverse-bias suppression is robust if we increase the interdot coupling Ω, whereas the forward-bias feature washes out as the three resonances start to overlap.

The reverse-bias CPT effect described here should be more robust with regards to dephasing induced by, e.g., background charge fluctuations than the dark state of the triple QD since it is substantially more localized. No interdot coherence is involved. Furthermore, the ease in tuning the magnetic field to precisely locate the dark state, as compared with the gate voltages in the triple QD, makes this an excellent setup for the further study of CPT and dark states in mesoscopic transport.

ACKNOWLEDGMENTS

This work was supported by the WE Heraeus Foundation and by DFG under Grants No. BR 1528/5-1 and No. GRK 1558.

APPENDIX: FULL COUNTING STATISTICS IN THE QUANTUM MASTER EQUATION

In this appendix, we give a brief review of the counting statistics formalism for quantum master equations as relevant to the DQD models discussed here. The original literature[10–12,16] should be consulted for more details.

Quantum dot systems weakly coupled to the leads are often described by a rate or quantum master equation of the form

$$\dot{\rho} = \mathcal{L}\rho, \quad (A1)$$

where $\mathcal{L}$ is the Liouvillian and ρ contains the relevant elements of the density matrix of the QD system—for a rate equation it contains just diagonal elements; in a quantum master equation, off-diagonal elements within charge sectors are also included.

It is convenient to arrange these density-matrix elements into a vector, such that the superoperator $\mathcal{L}$ takes matrix form. The stationary state of the system is then described by the vector $|\rho_{\mathrm{stat}}\rangle\rangle$, which is obtained as the right eigenvector: $\mathcal{L}\,|\rho_{\mathrm{stat}}\rangle\rangle = 0$. We assume this stationary state to be unique here. The corresponding left eigenvector of the Liouvillian, $\langle\langle\phi_0|\,\mathcal{L}=0$, has entries of unity at positions corresponding to populations and zero at those corresponding to coherences. Multiplication of an arbitrary "density-matrix-vector" $|\rho\rangle\rangle$ from the left with $\langle\langle\phi_0|$ is thus equivalent to taking the trace of ρ, and thus $\langle\langle\phi_0|\rho\rangle\rangle = \mathrm{Tr}\{\rho\} = 1$. For the 5×5 rate equations of Sec. II, this "trace" vector reads $\langle\langle\phi_0| = (1,1,1,1,1)$. We also define the steady-state "expectation value" $\langle\langle\mathcal{A}\rangle\rangle = \langle\langle\phi_0|\,\mathcal{A}\,|\rho_{\mathrm{stat}}\rangle\rangle = \mathrm{Tr}\{\mathcal{A}\rho_{\mathrm{stat}}\}$, for arbitrary superoperator $\mathcal{A}$.

1. *n*-resolved master equation

Consider that we are interested in the statistics of the electrons being transferred into the collector. With unidirectional (i.e., electrons can flow into the collector but not back out of it) single-electron current flow, the Liouvillian can be decomposed as

$$\mathcal{L} = \mathcal{L}_0 + \mathcal{J}, \quad (A2)$$

where superoperator $\mathcal{J}$ is that part of the Liouvillian which transfers an electron to the collector, and $\mathcal{L}_0$ leaves the number of electrons in the collector unchanged.

The solution of Eq. (A1) in Laplace-Liouville space is $\rho(z) = \Omega(z)\rho(t_0)$ with the propagator

$$\Omega(z) = [z - \mathcal{L}]^{-1} = [z - \mathcal{L}_0 - \mathcal{J}]^{-1}.$$

This latter we can expand as

$$\Omega(z) = \sum_{n=0}^{\infty} \Omega_0(z)[\mathcal{J}\Omega_0(z)]^n, \tag{A3}$$

with $\Omega_0(z)=[z-\mathcal{L}_0]^{-1}$. The density matrix in Laplace space is then $\rho(z)=\Sigma_{n=0}^{\infty}\rho^{(n)}$, with

$$\rho^{(n)}(z) = \Omega_0(z)[\mathcal{J}\Omega_0(z)]^n\rho(t_0). \tag{A4}$$

Since partial density-matrix $\rho^{(n)}(z)$ consists of a total of n jump operators acting (at various times) on the initial state, it represents that component of the density matrix with n electrons having been transferred to the collector.

Starting counting at $t=t_0$, the initial conditions read $\rho^{(0)}(t_0)=\rho(t_0)$ and $\rho^{(n)}(t_0)=0$ for $n\neq 0$, and from Eq. (A4) we can construct the following equations of motion for the n-resolved components:

$$\dot{\rho}^{(n)}(t) = \mathcal{L}_0\rho^{(n)}(t) + \mathcal{J}\rho^{(n-1)}(t), \tag{A5}$$

where it is understood that $\rho^{(-n)}=0$ for all n. Equation (A5) is the n-resolved master equation for our problem.

2. Counting field, χ

The equation set (A5) can be solved with a Fourier transform that introduces the *counting field* χ as the variable conjugate to n. We define

$$\rho(\chi;t) = \sum_n \rho^{(n)}e^{in\chi}. \tag{A6}$$

Multiplying Eq. (A5) with $e^{in\chi}$ and summing over n, we obtain the χ-resolved master equation

$$\dot{\rho}(\chi;t) = \mathcal{L}(\chi)\rho(\chi;t), \tag{A7}$$

with χ-dependent Liouvillian

$$\mathcal{L}(\chi) = \mathcal{L}_0 + e^{i\chi}\mathcal{J}, \tag{A8}$$

which is identical to original Liouvillian but with jump operator multiplied by counting factor $e^{i\chi}$.

3. Electron counting statistics

The moment and cumulant generating functions (MGF: $G(\chi;t)$ and CGF: $F(\chi;t)$) are defined as

$$G(\chi) = e^{F(\chi;t)} = \sum_{n=0}^{\infty} P(n;t)e^{in\chi}, \tag{A9}$$

where $P(n;t)$ is the probability of n electrons having been transferred to the collector after time t. The kth cumulant can be obtained as

$$\langle n^k\rangle_c(t) = \frac{\partial^k}{\partial(i\chi)^k}F(\chi;t)\big|_{\chi=0}. \tag{A10}$$

In the n-resolved approach, the probability of n electrons having passed to the collector after time t is simply

$$P(n;t) = \mathrm{Tr}\{\rho^{(n)}(t)\}, \tag{A11}$$

and the generating function is, therefore,

$$e^{F(\chi;t)} = \sum_{n=0}^{\infty} \mathrm{Tr}\{\rho^{(n)}(t)e^{in\chi}\} = \langle\langle\phi_0|\rho(\chi;t)\rangle\rangle, \tag{A12}$$

or in Laplace space

$$e^{F(\chi;z)} = \langle\langle\Omega(\chi,z)\rangle\rangle, \tag{A13}$$

where we have chosen the initial state to be the stationary state. Taking the long-time limit of this expression, the CGF simply becomes

$$F(\chi;t) \sim \lambda_0(\chi)t, \tag{A14}$$

where $\lambda_0(\chi)$ is that eigenvalue of $\mathcal{L}(\chi)$, which tends to zero as $\chi\to 0$.

Often, we are only interested in the first few current cumulants, or it may be that the complete diagonalization of $\mathcal{L}(\chi)$ to obtain $\lambda_0(\chi)$ is beyond us. In such cases, Eq. (A13) can be expanded as a function of χ and the derivatives taken directly. From this, the following expressions for the (stationary) average current and shot noise can be obtained:

$$\langle I\rangle = \langle\langle\mathcal{J}\rangle\rangle \tag{A15}$$

$$S = \langle\langle\mathcal{J}\rangle\rangle + 2\langle\langle\mathcal{J}\mathcal{R}(0)\mathcal{J}\rangle\rangle, \tag{A16}$$

where $\mathcal{R}(z)$ is the pseudoinverse $\mathcal{R}(z)=\mathcal{Q}[z-\mathcal{L}(0)]^{-1}\mathcal{Q}$ with $\mathcal{Q}=\mathbb{1}-\mathcal{P}$ and $\mathcal{P}=|\rho_{\mathrm{stat}}\rangle\rangle\langle\langle\phi_0|$.

[1] C. Payette, G. Yu, J. A. Gupta, D. G. Austing, S. V. Nair, B. Partoens, S. Amaha, and S. Tarucha, Phys. Rev. Lett. **102**, 026808 (2009).

[2] L. P. Kouwenhoven, D. G. Austing, and S. Tarucha, Rep. Prog. Phys. **64**, 701 (2001).

[3] B. Michaelis, C. Emary, and C. W. J. Beenakker, EPL **73**, 677 (2006).

[4] C. W. Groth, B. Michaelis, and C. W. J. Beenakker, Phys. Rev. B **74**, 125315 (2006).

[5] C. Emary, Phys. Rev. B **76**, 245319 (2007).

[6] C. Pöltl, C. Emary, and T. Brandes, Phys. Rev. B **80**, 115313 (2009).

[7] H. Sprekeler, G. Kießlich, A. Wacker, and E. Schöll, Phys. Rev. B **69**, 125328 (2004).

[8] We have repeated these calculations with a coherent treatment of the interdot coupling and with internal coherences included in the density-matrix $\rho(t)$. For $T\gg\Gamma,\gamma$, the results are in close agreement with those from the rate equation approach. This validates the use of this simpler approach in the experimentally relevant regime.

[9] L. S. Levitov and G. B. Lesovik, JETP Lett. **78**, 230 (1993); L. S. Levitov, H. W. Lee, and G. B. Lesovik, J. Math. Phys. **37**, 4845 (1996).

[10] D. A. Bagrets and Yu. V. Nazarov, Phys. Rev. B **67**, 085316

(2003).
[11] C. Flindt, T. Novotný, and A.-P. Jauho, Phys. Rev. B **70**, 205334 (2004); C. Flindt, T. Novotný, and A.-P. Jauhoa, Physica E (Amsterdam) **29**, 411 (2005); A.-P. Jauho, C. Flindt, T. Novotný, and A. Donarini, Phys. Fluids **17**, 100613 (2005); C. Flindt, T. Novotný, A. Braggio, M. Sassetti, and A.-P. Jauho, Phys. Rev. Lett. **100**, 150601 (2008).
[12] C. Emary, Phys. Rev. B **80**, 235306 (2009).
[13] Ya. M. Blanter and M. Büttiker, Phys. Rep. **336**, 1 (2000).
[14] D. Jacob, B. Wunsch, and D. Pfannkuche, Phys. Rev. B **70**, 081314(R) (2004).
[15] A. Cottet, W. Belzig, and C. Bruder, Phys. Rev. Lett. **92**, 206801 (2004); Phys. Rev. B **70**, 115315 (2004); A. Cottet and W. Belzig, EPL **66**, 405 (2004); W. Belzig, Phys. Rev. B **71**, 161301(R) (2005).
[16] R. J. Cook, Phys. Rev. A **23**, 1243 (1981).